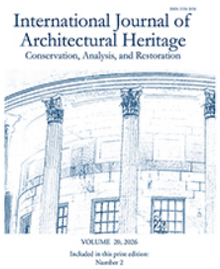

International Journal of Architectural Heritage
Conservation, Analysis, and Restoration

ISSN: 1558-3058 (Print) 1558-3066 (Online) Journal homepage: www.tandfonline.com/journals/uarc20

Full-Scale Simulated Seismic Field-Testing of a Post-Tensioned Glue Laminated Timber Portal Frame Structure Deploying Traditional Māori Construction Techniques

Sonny Vercoe, Anthony Hōete, Jason Ingham & Sherif Beskhyroun

To cite this article: Sonny Vercoe, Anthony Hōete, Jason Ingham & Sherif Beskhyroun (24 Feb 2026): Full-Scale Simulated Seismic Field-Testing of a Post-Tensioned Glue Laminated Timber Portal Frame Structure Deploying Traditional Māori Construction Techniques, International Journal of Architectural Heritage, DOI: 10.1080/15583058.2025.2598035

To link to this article: https://doi.org/10.1080/15583058.2025.2598035

INTERNATIONAL JOURNAL OF ARCHITECTURAL HERITAGE
https://doi.org/10.1080/15583058.2025.2598035

Taylor & Francis
Taylor & Francis Group

RESEARCH ARTICLE

OPEN ACCESS Check for updates

Full-Scale Simulated Seismic Field-Testing of a Post-Tensioned Glue Laminated Timber Portal Frame Structure Deploying Traditional Māori Construction Techniques

Sonny Vercoe[a], Anthony Hōete[b], Jason Ingham[c], and Sherif Beskhyroun[d]

[a]Faculty of Engineering and Design, University of Auckland; [b]Professor of Architecture (Māori), Faculty of Engineering and Design, University of Auckland; [c]Professor of Structural Engineering, Faculty of Engineering and Design, University of Auckland; [d]Professor of Structural Engineering, Faculty of Design & Creative Technologies, Auckland University of Technology

ABSTRACT

Testing was undertaken to investigate the viability of a traditional Māori post-tensioned construction technique that incorporated modern glue-lamination manufacturing to withstand seismic loadings. A feature of the form-fit connections was that the timber members were seated into pockets. A companion numerical model was developed to confirm aspects not readily measured in the field. Vertical loading was applied at the apex via water-filled containers. Seismic loading was simulated by applying a horizontal loading system at the apex via a winch and quick-release system, involving seven pseudo-static semi-cyclic tests followed by three snap-back tests. It was established that member demands remained within capacity, that apex vertical and horizontal displacements remained within code-defined deflection limits, and that the measured damping was 7.3%. Findings are also reported for mode shapes and joint rotational stiffness. Novel aspects of the reported research included full-scale field testing at a remote site, collaborations with the local indigenous Māori community, the incorporation of both traditional and modern post-tensioned timber construction techniques, and the intentional use of a methodology for simulated loading which could be undertaken within a community setting.

ARTICLE HISTORY
Received 17 July 2025
Accepted 26 November 2025

KEYWORDS
Full-scale field test; indigenous Māori construction; numerical model calibration; post-tensioned timber portal frame; simulated seismic response; snap back testing

1. Introduction

1.1. Background

Traditional indigenous meeting houses in New Zealand are referred to by Māori as wharenui (whare → house, nui → large) in te reo Māori (the Māori language). Meeting houses have significant historical, social and architectural value for Māori (Hoete 2020). There is pre-colonial evidence of Māori using post-tensioning techniques (mīmiro) for the construction of wharenui within the Ngāti Awa rohe (region). Adapted from boat-building techniques, mīmiro was an endangered traditional Māori construction technique that offered structural stability not previously tested in a seismic setting.

In 1874, this technique was deployed by Ngāti Ira for their own ancestral house, Tānewhirinaki (Figure 1). Located in the Waioweka, in the eastern Bay of Plenty region of New Zealand (Figure 2(b)), this is an area prone to a range of natural hazards. Following a series of reconstruction failures in its earlier years, coupled with the 1886 Mt Tarawera eruption (Ngāti Ira 2022; Wikipedia 2024a) and 1931 Hawkes Bay earthquake (Ngāti Ira 2022; Wikipedia 2024b), the structural stability of this traditional meeting house was compromised. This historically innovative wharenui, a structural manifestation of both traditional Māori and colonial technologies, was subsequently dismantled and stored.

Like Tānewhirinaki, many wharenui need heritage conservation and would benefit from resilient construction to better support and protect their communities. The testing of a post-tensioned structure is, thus, part of an ongoing programme of research with tangata whenua (people of the land) (Hoete 2025). This research seeks to enable, support, and enhance the heritage value of wharenui and historical structures alike through the revival of traditional post-tensioning techniques to increase seismic resilience across Aotearoa New Zealand.

1.2. Post-tensioned timber construction (mīmiro)

An extensive number of studies have been published on the experimental testing of post-tensioned timber structures (Yeap and Yeoh 2022), with some of that research

CONTACT Sonny Vercoe sver160@aucklanduni.ac.nz Faculty of Engineering and Design, University of Auckland

Figure 1. Tāne Whirinaki in 1920s. Photograph taken by Charles Troughton Clark circa 1913. Reproduced with permission of the National Library of New Zealand. Reference: PAColl-0477–01.

undertaken locally in New Zealand (Buchanan et al. 2009; Iqbal, Pampanin, and Buchanan 2021; Kasal et al. 2004; Moroder, Buchanan, and Pampanin 2013; Palermo et al. 2005, 2011; Smith et al. 2012, 2014; Spellman et al. 2012). A limited number of previous studies have also been published on the experimental seismic testing of full-scale timber portal frames, primarily focusing on the performance of joints (Komatsu 1993, 2017; Komatsu and Mori 2006; Noguchi, Takino, and Komatsu 2006; Zhang et al. 2019), the behaviour, and performance of bracing (Liu and Xiong 2018; Ni et al. 2014; Xiong and Liu 2016), and strengthening (Chang and Hsu 2010; Kasal et al. 2004). However, studies combining post-tensioning with timber portal frames are notably lacking. The study undertaken by Shahmohammadi et al. (2022) involved the full-scale seismic field-testing of a steel portal frame and is acknowledged to have contributed to the conceptualisation of the testing reported herein.

1.3. Site location and ground conditions

The testing was undertaken on a 2,700 m^2 land section near Ōpōtiki in the eastern Bay of Plenty region of New Zealand, as shown in Figure 2(c). It was positioned adjacent to Ōpeke marae (complex of Māori buildings), Waioweka Primary School (Te Kura o Waioweka, kura → school) and the surrounding village (papakāinga). A marae is a complex of Māori buildings that serves as a place of belonging (tūrangawaewae) for its tribe and that primarily include the meeting house (wharenui), dining hall (wharekai), and ablution blocks (wharepaku) among other buildings. Occupying approximately 1,400m^2 (when accounting for the test unit, field-testing trailer and loading equipment), the test site was clear and flat, with a falling gradient of 1:70 (south to north).

Ground conditions were determined via a desktop investigation, hand shear vane testing, and results from existing geotechnical investigations. The desktop investigation involved assessing the interactive geological map of New Zealand (GNS Science 2024), which showed the surface distribution of geological units at scales of 1:250K and 1:1 M, indicating that the test site was likely comprised of gravel, sand, silt, mud, and clay, with local occurrences of peat. Hand shear vane testing was undertaken within the test operations area to determine the peak undrained shear strengths (s_u). The ultimate bearing capacity (q_u) was determined using the Verification Method B1/VM4 Foundations (Ministry of Business, Innovation & Employment 2023), which confirmed that the test site ground conditions complied with the NZS 3604 definition for good ground (Standards New Zealand 2011). An earlier geotechnical investigation by Engineering Design Consultants Limited (2023) had also been undertaken at the neighbouring complex of Māori buildings (marae) located within 100 m of the test site. As shown in Figure 2(d), this investigation included shallow intrusive hand augering at nine exploratory locations with the associated scalar penetrometer and shear vane testing undertaken up to a depth of 3.1 m. Similar to the result of hand shear vane testing, the findings from this earlier geotechnical investigation confirmed that the neighbouring complex of Māori buildings (marae) was also founded on good ground.

(a) *Map of New Zealand showing locations of interest on the North Island*

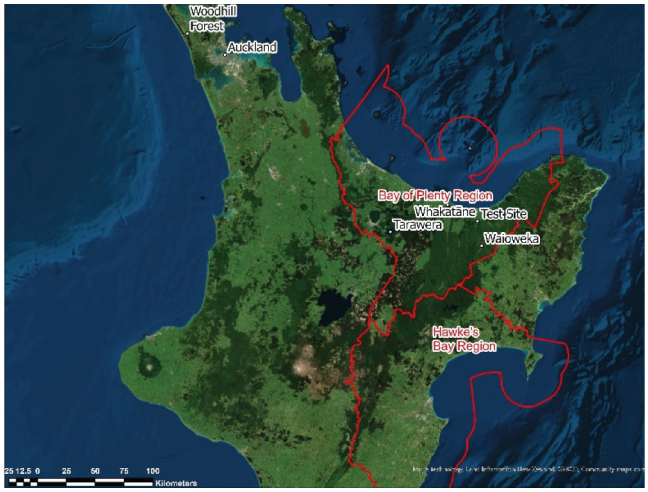

(b) *Map of North Island showing all locations of interest*

(c) *Map of test site*

(d) *Locations of hand auger holes (Engineering Design Consultants Limited, 2023)*

(e) *Undertaking hand shear vane testing*

Figure 2. Site location and geotechnical investigation plan.

2. Materials and methods

2.1. Test unit design

As shown in Figure 3, the overall dimensions of the test unit were a width of 13.87m measured at the base, a height of 6.49m at the apex, and a depth of 3.05m. The test unit incorporated three GL8 glue laminated (glulam) timber portal frames at 1.25 m centre spacings (see Figure 3(b)), with the six columns (poupou) having cross-section dimensions of 550 mm × 135 mm (see Figure 3(c)), the six rafters (heke) having a half-round cross-section with a diameter of 330 mm (see Figure 3(d)), the four purlins (kaho) having a cross-section of 150 mm × 300 mm (see Figure 3(a)), and the ridge beam (tāhuhu) having a cross-section of 650 mm × 200 mm (see Figure 3(e)). As shown in Figure 3(f), the test unit featured 20 MPa concrete strip footing foundations with a width of 360 mm, a height of 900 mm, and a depth of 3250 mm. The concrete was reinforced with 4-D12 longitudinal bars and D12 open-loop stirrups at centres of 650 mm and 600 mm, respectively. Member sizing was an exercise led by Hōete. Since the test unit was to be dismantled immediately after testing, it was decided that embedding the columns (poupou) into the concrete foundation without a capillary break was sufficient for testing purposes. It is acknowledged that the durability of the permanent structure would be governed by the sensitivity of the columns (poupou)

to the water capillary action in the concrete (Hoete 2025).

2.2. Test unit assembly

While positioned at their intended spacing, the columns (poupou) were fitted with a backing frame so that it could be readily reapplied at the test site (see Figure 6 (a)). All members were then disassembled and transported to the test site using the dedicated field-testing trailer (see Figure 6(b)).

The assembly of the test unit at the test site was coordinated by Hōete and was completed in two phases. The first phase occurred between 9 and 10 February 2023 and involved excavating the footings intentionally using manual labour, installing the columns (poupou), and positioning the foundation reinforcement ready for concrete placement. A topographical site survey was undertaken to ensure the precise demarcation of the foundation boundary and accurate placement of the columns (poupou). After the footings were excavated by hand as shown in Figure 4(c), the columns (poupou) were remounted on the backing frames to ensure uniform spacing and were fixed to the scaffold support structure to ensure correct alignment and orientation (see Figure 4(d)). Once the columns (poupou) were positioned correctly the foundation reinforcement was placed, with the longitudinal reinforcement being held in position by temporary bars driven into the walls of the excavated footings that also

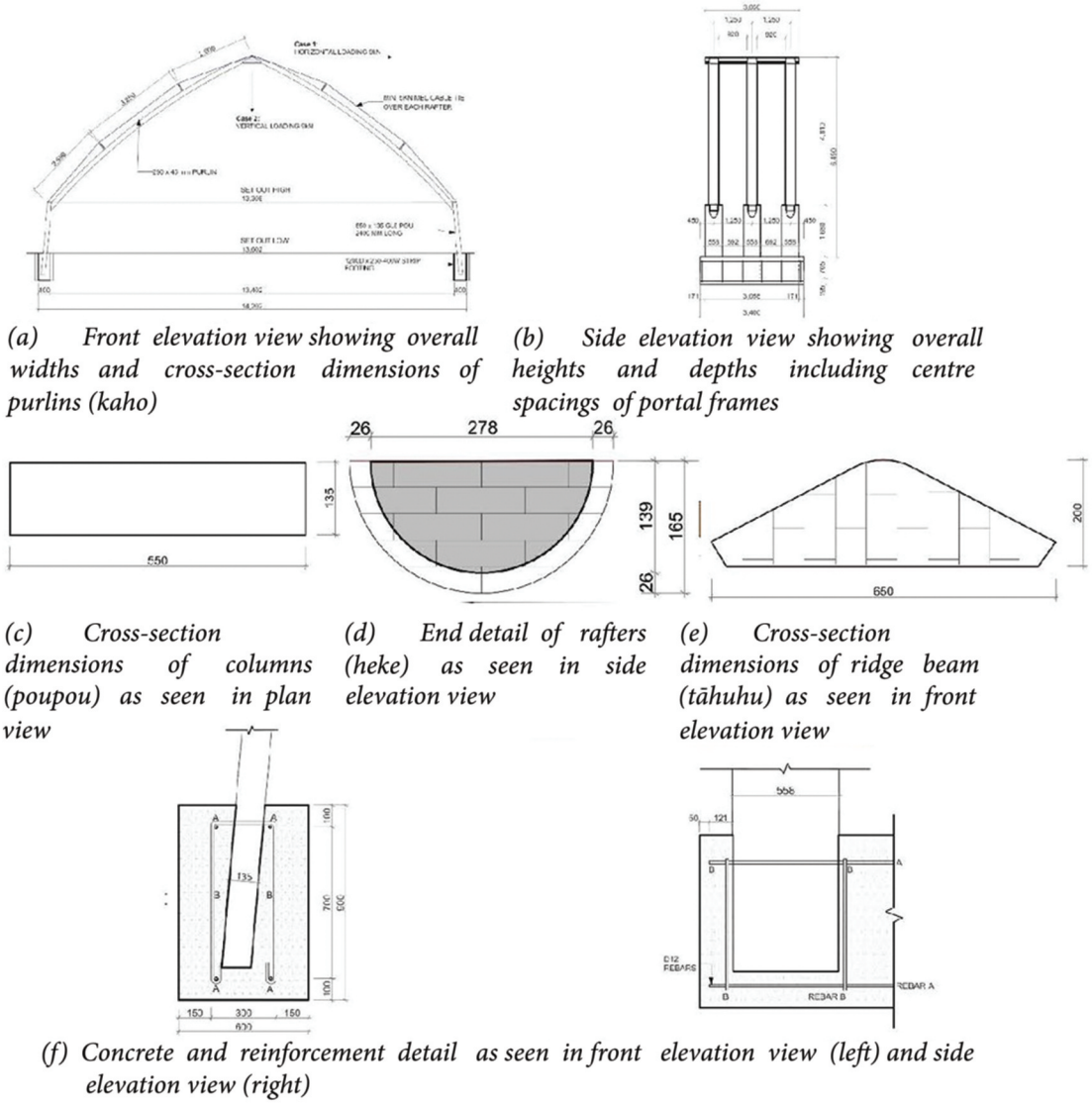

(a) Front elevation view showing overall widths and cross-section dimensions of purlins (kaho)

(b) Side elevation view showing overall heights and depths including centre spacings of portal frames

(c) Cross-section dimensions of columns (poupou) as seen in plan view

(d) End detail of rafters (heke) as seen in side elevation view

(e) Cross-section dimensions of ridge beam (tāhuhu) as seen in front elevation view

(f) Concrete and reinforcement detail as seen in front elevation view (left) and side elevation view (right)

Figure 3. Dimensions of test portal and individual elements, Design and drawings produced by Anthony Hōete.

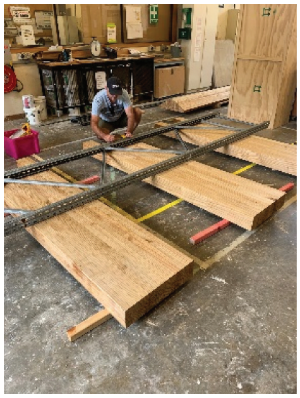

(a) Mounting columns (poupou) onto backing frames in UoA architectural laboratory

(b) Field-testing trailer used to transport columns (poupou) to test site

(c) Footings dug by hand

(d) Positioning of columns (poupou) prior to concrete placement

Figure 4. Preparation and positioning of columns (poupou) and foundations.

provided a resting platform for the stirrups. Concrete was sourced from a commercial ready-mixed concrete supplier and the foundation was given 28 days to cure.

The second phase of assembly involved the installation of the rafters (heke), ridge beam (tāhuhu) and purlins (kaho). A scaffold structure was erected to provide a temporary resting platform to support the ridge beam (tāhuhu). The rafters (heke) were then lowered and held in position to scarf and bolt into the ridge beam (tāhuhu) and notch into the columns (poupou), intentionally using manual labour to replicate traditional construction practices.

After all test unit members were assembled the components of the post-tensioning system were installed as shown in Figure 5. Mīmiro's seafaring origin was recognised by intentionally sourcing all-post-tensioning hardware from the maritime sailing industry; ⌀10 mm double braid rope (Fosters Chandlery 2024a) as the post-tensioning cable, high-load exit boxes (Ronstan International Pty Ltd 2024) for rope redirection, a swivel block (Harken New Zealand, Limited 2024b) to connect the dead end anchorage and live end and a rope clutch (Spinlock Limited 2024) to secure the post-tensioned cable. In addition, a single-speed winch (Harken New Zealand, Limited 2024a) and lock-in handle (Harken New Zealand, Limited 2024d) combined with pad eyes (Harken New Zealand, Limited 2024c) and horn cleats (Fosters Chandlery 2024b) were used for tension adjustment. The post-tensioning system was also equipped with load cells (VPG Force Sensors 2024) for data acquisition. The post-tensioning force of 2 kN was established after manually operating the winch with the maximum effort achievable by a member of the research team.

(a) High-load exit box mounted on ridge beam (tāhuhu)

(b) Rendered view of live end and clutch

(c) Dead end anchorage

(d) Waterproofing of compromised load cell

Figure 5. Post-tensioning (mīmiro) system.

The rope sourced from Fosters Chandlery (Fosters Chandlery 2024a) in Auckland was ⌀10 mm with a specified spliced breaking load of 24.5 kN. A 20-m length of this rope was tested in the UoA Structures Test Laboratory (STL) following the completion of a safe work method statement (SWMS) and associated risk assessment. As shown in Figure 6, a load cell was connected to the rope and the rope was tied to a forklift at one end and anchored to a large concrete block at the other end. The data logger recorded rope failure at 4.6 kN (19% of specified breaking load), with failure occurring at the knot and resulting in a stretch of approximately 1 m (5% elongation). This rope pull-test demonstrated that the capacity at the location of the knot was substantially less than the specified breaking strength, but that the intended post-tensioning force of 2 kN was well below the knot breaking strength of the rope. It was also concluded that the low stiffness (high elongation) of the rope would result in little increase in post-tensioning force during simulated seismic excitation of the test structure.

2.3. Design loading and code-defined displacement limits

Wharenui are typically adorned with hand-crafted carvings throughout their structure. A simplified lumped mass model was assumed, where the dead load of the absent roof and carvings acting over the central 50% of the span between the semicircular knee joints (ruawhetū) was concentrated at the tāhuhu (ridge beam). This supplementary dead load mass was estimated to be 14.15 kN as calculated in Table 1. A roof live load of 0.25 kPa was considered for the structure based on the R2 category of NZS 1170.1 (Standards New Zealand 2002b), which accounted for structural elements supporting the cladding. Using the same

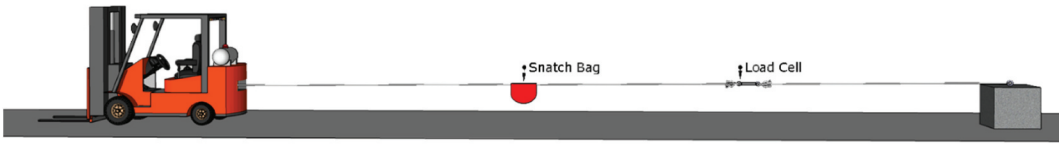

(a) Rendered view of rope pull-test

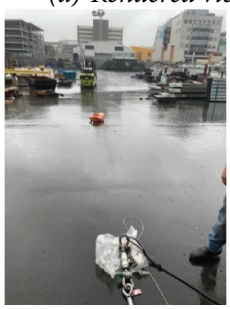

(b) Rope pull-test setup

(c) Rope showing break location at the knot

(d) Frayed end of broken rope

Figure 6. Testing of rope in the STL.

Table 1. Design loading calculations.

Parameter	Value
Absent roof plan dimensions	10.88 m × 24.3 m
Absent roof total mass	10,695 kg
Portal frame centre spacing	1.25 m
Tributary width of three rafters (heke)	3 × 1.25 = 3.75 m
Mass per carving	127 kg
Number of portal frames in proposed new and resilient meeting house (wharenui)	19
Total mass of carvings	(19–1) × 2 × 127 = 4572 kg
Total mass acting over central 10.880 m of the structure	10,695 + 4572 = 15,267 kg
Total mass acting over tributary width of three rafters (heke)	15,267 × 3.75/24.3 = 2356 kg
Semicircular knee joint (ruawhetū) span	0.5 × 13.308 = 6.654 m
Simplified dead load (G)	2,356 × 6.654/10.880 × 9.81/1000 = 14.15 kN
Roof live load	0.25 kPa
Simplified live load (Q)	0.25 × 6.654 × 3.75 = 6.24 kN
NZS 1170.0 serviceability vertical load combination (G+0.7Q)	14.15 + 0.7 × 6.24 = 18.52 kN
NZS 1170.0 vertical strength and stability load combination (1.2G + 1.5Q)	1.2 × 14.15 + 1.5 × 6.24 = 26.34 kN

procedure as described above, a simplified lumped mass for the roof live load was estimated to be 6.24 kN as calculated in Table 1. NZS 1170.0 serviceability vertical loading was estimated to be 18.52 kN (this scenario not tested in the field) and NZS 1170.0 vertical strength and stability were estimated to be 26.34 kN (again, this scenario was not tested in the field) as calculated in Table 1 (Standards New Zealand 2002a). For both dead and live loads the remaining tributary loads to be concentrated at the semicircular knee joints (ruawhetū) were neglected because vertical loading of the columns (poupou) was not a critical concern due to their large cross-sectional area.

Seismic loading was calculated for the NZS 1170.0 load combination G + 0.3Q & E_u as shown in Table 2. The dead load incorporated the roof structure and the absent roof and carvings Figure 7. The roof structure comprised a127 kg ridge beam (tāhuhu) and six 172 kg rafters (heke) corresponding to a roof structure dead load of 11.37 kN as calculated in Table 2. The dead load of the absent roof and carvings acting over the central 50% of the span between the semicircular knee joints (ruawhetū) was previously estimated to be 14.15 kN and hence the dead load acting over the remainder of the roof was estimated to be 8.96 kN as calculated in Table 2. Consequently, the total dead load contributing to the seismic mass was G = 34.48 kN as calculated in Table 2. Similarly, the live load acting over the central 50% of the span between the semicircular knee joints (ruawhetū) was previously estimated to be 6.24 kN and the live load acting over the remainder of the roof was estimated to be 3.96 kN as calculated in Table 2. Consequently, the total live load contributing to the seismic mass was Q = 10.21 kN, and the corresponding seismic mass was 37.54 kN as calculated in Table 2.

Table 2. Seismic loading calculations.

Parameter	Value
Roof structure dead load	(127 + 6 × 172) × 9.81/1000 = 11.37 kN
Dead load acting over remainder of roof	2,356 × (10.88 - 6.654)/10.88 × 9.81/1000 = 8.96 kN
Total dead load contributing to seismic mass (G)	11.37 + 14.15 + 8.96 = 34.48 kN
Live load acting over remainder of roof	0.25 × 4.226 × 3.75 = 3.96 kN
Total live load contributing to seismic mass (Q)	6.24 + 3.96 = 10.21 kN
Seismic mass (G + 0.3Q)	34.48 + 0.3 × 10.21 = 37.54 kN

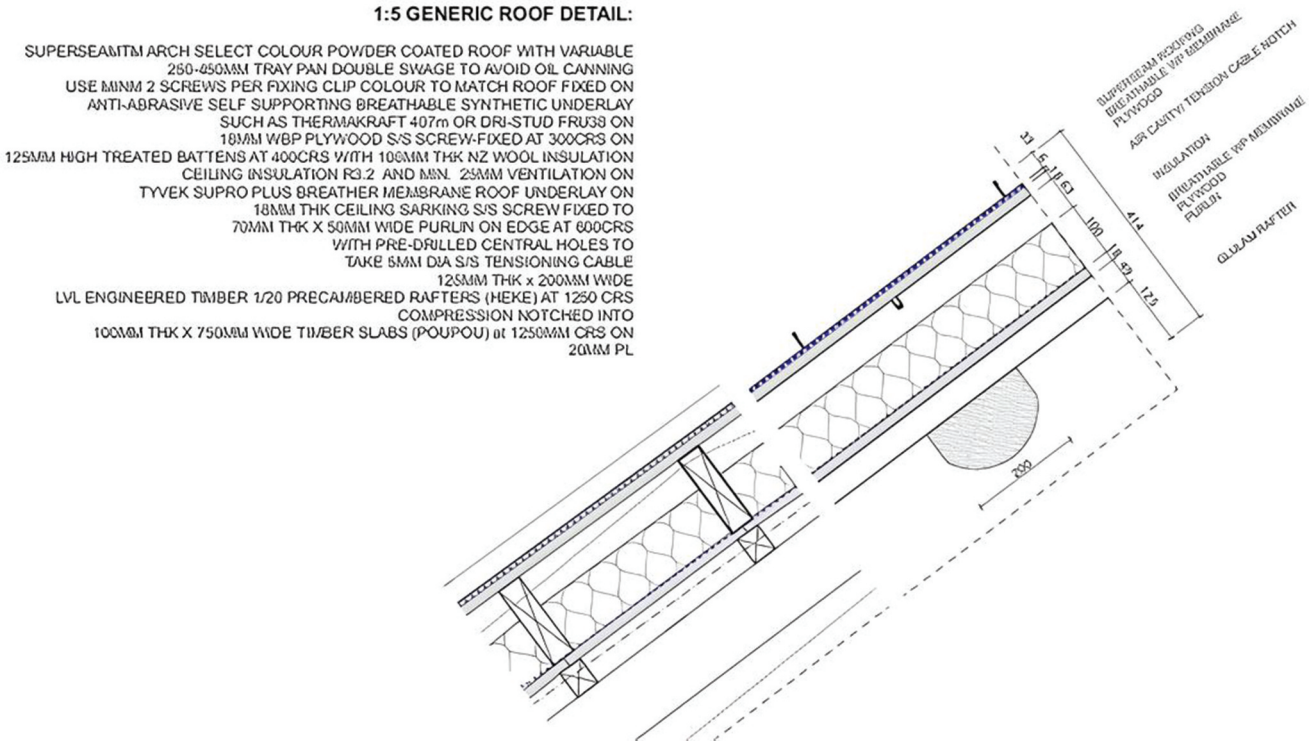

Figure 7. Detail showing roof build up. Design and drawing produced by Anthony Hōete.

The design earthquake load (E_u) of 34.6 kN was evaluated as a single equivalent static force using the equivalent static analysis method in NZS 1170.5 (Standards New Zealand 2004) as calculated below in Table 3. The hazard factor (Z) for Ōpōtiki was 0.30 and a first-mode period (T_1) of 0.37 s was determined via a companion numerical model described later. Because the stiffness characteristics of the semicircular knee joints (ruawhetū) were unknown the joints were assumed to be pinned, but because the forecast period was on the plateau of the design spectra the design level loading was not sensitive to the adopted first mode period. Because the structure was single-storey E_u was equal to the base shear (V). With a seismic weight (W_t) equal to the design vertical load (37.54 kN), the design-level base shear force V was established to be 34.6 kN as calculated below in Table 3.

The permitted vertical deflection of the roof was based on the NZS 1170.0 suggested serviceability vertical deflection limit. For roof-supporting elements subjected to $G + \Psi_l Q$ (dead load plus long-term live load) this limit was span/300 where span is defined in NZS 1170.0 as the clear spacing between the points of support. The points of roof support were at the semicircular knee joints (ruawhetū) and hence the span was 13.308 m and the limit was estimated to be 13,308/300 = 44 mm. Because the long-term combination factor is $\Psi_l = 0$ the total vertical loading to be applied at the apex was G = 14.15 + 0 × 6.24 = 14.15 kN. The permitted horizontal deflection of the roof was based on the NZS 1170.5 ULS inter-storey deflection limit of 2.5%. Because the test structure was single-storey structure with a height to the apex of 6.49 m, the horizontal deflection limit was 0.025 × 6,490 = 162 mm.

Table 3. Design earthquake load calculations.

Parameter	Value
Importance level	3
Site subsoil class	C
Design working life	50
Annual exceedance probability	1/1000 yr^{-1}
Ultimate limit state return period factor (R_U)	1.3
Near fault factor (N(T,D))	1
Hazard factor (Z)	0.3
First mode period (T_1)	0.37 s
Spectral shape factor ($C_h(T)$)	2.36 g
Elastic site hazard spectrum for horizontal loading ($C(T_1)$)	$2.36 \times 0.3 \times 1.3 \times 1 = 0.92$ g
Structural ductility factor (μ)	1
Inelastic spectrum scaling factor (k_μ)	1
Structural performance factor (S_p)	1
Seismic weight (G + 0.3Q)	$34.48 + 0.3 \times 10.21 = 37.54$ kN
Horizontal seismic base shear (V_e)	$0.92 \times 37.54 = 34.6$ kN
Ultimate limit state earthquake action (E_u)	34.6 kN

2.4. Instrumentation and weather protection

Testing was initially postponed to 15 March 2023 because of delays encountered with the manufacture of the curved rafters (heke) due to equipment breakdown at the timber milling operation, resulting in late delivery of the rafters (heke). Testing was then postponed again to 30 March 2023 because of further machinery problems associated with the manufacture of the curved rafters (heke). Testing was postponed for a third time because of a funeral (tangihanga) at Ōpeke marae (complex of Māori buildings positioned adjacent to the test site) and UoA campus commitments once lectures had commenced for the semester. Testing was eventually completed between 21 and 23 April 2023.

The repeated postponements described above resulted in no further delays being permissible and unfortunately the weather turned foul as testing commenced (see Figure 8). Efforts made to protect all instrumentation from the inclement weather using plastic containers and plastic bags were successful except for (i) the load cell in Figure 5(d) which was to be used to measure the post-tensioning force on one portal frame; and (ii) the load cell in the simulated seismic loading system described later which was to be used to measure the force in the wire rope. Because post-tensioning load cells were installed on each of the three portal frames, the post-tensioning force was measured using the two remaining operational load cells and comparable tension in the compromised post-tensioned cable was manually judged on-site. Figure 8 also shows site personnel equipped with rainwear. The instrumentation coding is reported in Figure 8(e), showing displacement sensors placed at nine locations along the test unit to measure vertical and horizontal displacements.

The field-testing trailer that was initially used to transport the columns (poupou) and backing frames during test unit assembly (see Figure 4(b)) acted as a mobile office during testing and was a safe lockable overnight storage facility for the data acquisition and test site equipment as shown in Figure 9(b). The field-testing trailer was generator-powered, had mobile Wi-Fi functionality and was equipped with sliding glass windows to allow visual monitoring as testing progressed. The field-testing trailer also featured a pass-through wall port that was used to run cables from the displacement sensors to the data acquisition station as shown in Figure 9(b).

2.5. Verification of field-testing equipment

Because the test site (see Figure 2(c)) was located approximately 350 km from the University of Auckland (UoA) campus (also referred to as home base) it was recognised that it would be beneficial to trial the installation of vertical loading. Furthermore, some members of the research team had limited experience with structural testing and aspects to consider when operating in the field. As reported previously, the required supplementary vertical loading was calculated to be 14.15 kN for the $G + \Psi_l Q$ load combination. Based upon past successful testing by Shahmohammadi et al. (2022) a decision was made to use Intermediate Bulk Containers (IBCs) filled with water to provide the supplementary vertical load to imitate the absent roof and carvings. Two 1000 L IBCs were purchased, each having a mass of 60 kg and therefore a maximum storage mass of $(2 \times 1060) \times 9.81/1000 = 20.8$ kN. New slings were purchased specifically for the project, and a mock-up of the ridge beam (tāhuhu) was assembled on 3 February 2023

(a) Footing in the rain

(b) Test unit in the rain

(c) Site personnel in rainwear, showing weatherproofing of instrumentation on columns (poupou)

(d) Weatherproofing of displacement sensors

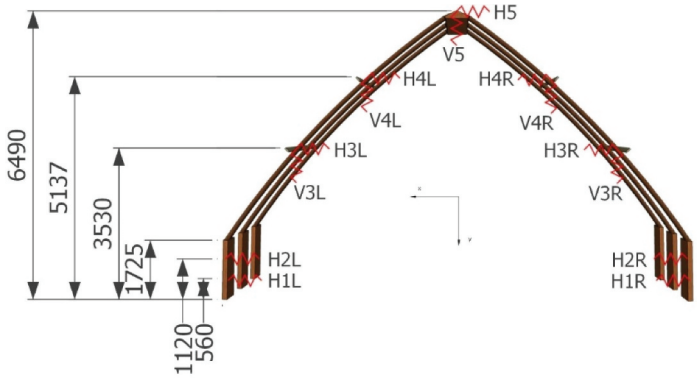

(e) Notation and locations of displacement sensors

Figure 8. Testing weather conditions and displacement sensors.

(a) Field-testing trailer being locked overnight after testing

(b) Data acquisition station in operation during testing

Figure 9. Field-testing trailer used during testing.

(a) Mock up of ridge beam (tāhuhu) with slings

(b) Proposed vertical load system trialled in UoA STL

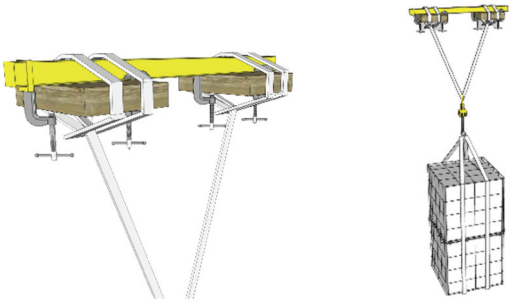

(c) Rendered views of the proposed vertical load system

Figure 10. Field-testing equipment.

(a) Data acquisition station at 4WD park

(b) View of mock-up loading of rotten stump

Figure 11. Verification testing at 4WD park.

using the gantry crane in the UoA Structures Test Laboratory (STL) as shown in Figure 10.

A decision was also made to trial the installation procedure for the simulated seismic loading at the regional four-wheel drive (4WD) park in Woodhill Forest (Auckland Off Road Adventure 2024) on 4 February 2023. One reason for the trial was to check that all necessary equipment was considered and accounted for. Furthermore, some members of the research team had limited experience with data acquisition and hence the trial allowed members of the research team to practise data capture with the data logger in the field as shown in Figure 11(a). Risk assessment and field activity plans were completed, and the park administrators were informed and approved the planned activity. Because it was unlawful to damage a living tree, a rotten stump located well away from other park users was selected as a suitable practice test unit as shown in

Figure 11(b). All equipment was carefully laid out, including safety signage on the approaches to the test site. The trial was successful, with no problems encountered.

2.6. Vertical loading system

The on-site vertical loading system incorporated several variations to address site safety considerations, including that the IBCs were stacked horizontally instead of vertically to remain closer to the ground and represent a lower risk of tumbling, and that a chain block was employed to conveniently raise and lower the IBCs at the beginning and end of testing cycles, as shown in Figure 12(a). Water was pumped from the nearby stream and flow-metered hoses were used to transfer water to the IBCs in known quantities. Vertical loading was achieved via the IBC load system to apply the supplementary vertical load of 14.15 kN, and unloading by releasing water from the IBC outlets onto the ground was considered unnecessarily wasteful such that at the conclusion of testing each day the IBCs were instead carefully lowered to the ground with the chain blocks.

3. Results

3.1. Simulated seismic loading

The components of the simulated seismic loading system shown in Figure 13 were a winch rated for 44.5 kN mounted to a 2021 Jeep Gladiator Sport (Jeep), a dual-stage 12:1 pulley system, and anchorage restraints provided by 5 parked vehicles and two 1 m^3 concrete blocks. In the first stage of the simulated seismic loading system the winch cable passed through three snatch blocks at the dead end adjacent to the concrete block and through two snatch blocks at the live end adjacent to the Jeep, with the cable tied back to the Jeep to generate a 6:1 load-amplification configuration (see Figure 13(a)). In the second stage of the simulated seismic loading system, a wire rope (connected to the first stage) was passed through an additional snatch block located adjacent to the test unit apex that was then returned and tied off to the front anchorage point, generating the 12:1 load-amplification configuration. For simplicity, the rendered view in Figure 13(a) shows a flat site, whereas in reality the site sloped downhill towards the front anchorage. Assuming a site descent of 1 m and accounting for the 1 m height of the concrete block, the rope angle was determined to be $\theta = \tan^{-1}((6.49 - 1 + 1)/(5 + 15 + 6.935)) = 16.5°$.

Simulated seismic testing included seven pseudo-static semi-cyclic tests with imposed horizontal displacements of approximately 10 mm, 20 mm, 30 mm, 40 mm, 50 mm, 60 mm, and 70 mm, followed by three quick-release snap back tests at release horizontal displacements of approximately 50 mm, 60 mm, and 70 mm.

The snap-back simulated seismic response was consistent across all tests and all horizontal displacement gauges, as shown in Figure 14(a-c), confirming the high fidelity of the recorded horizontal data. The snap back vertical response was also consistent except for sensor V5 (located at the ridge beam (tāhuhu), see Figure 8(e)) as shown in Figure 14(d-f). It was suspected that because the IBCs were suspended from the ridge beam (tāhuhu), and because the simulated seismic loading system was fixed to the ridge beam (tāhuhu) and applied a minor vertical component of load ($\tan(16.5°) = 0.30F$) due to the non-horizontal orientation of the simulated seismic loading system, sensor V5 was likely disrupted by the vertical bouncing motion of the IBCs following the snap back quick release.

(a) Rendered isometric view (b) Filling IBCs with water (c) Vertical loading system during vertical test

Figure 12. Vertical loading system.

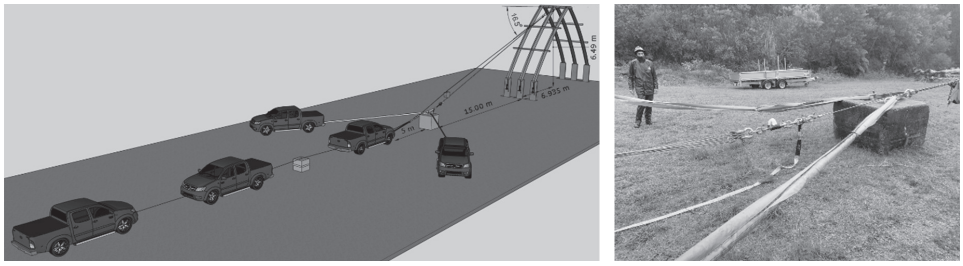

(a) Rendered view showing vehicles, rope angle and distances

(b) Pulley system

(c) On-site view showing the ve hicles, front concrete anchorage and pulley system

(d) On-site view showing the test unit

Figure 13. Rendered and on-site view of simulated seismic loading system.

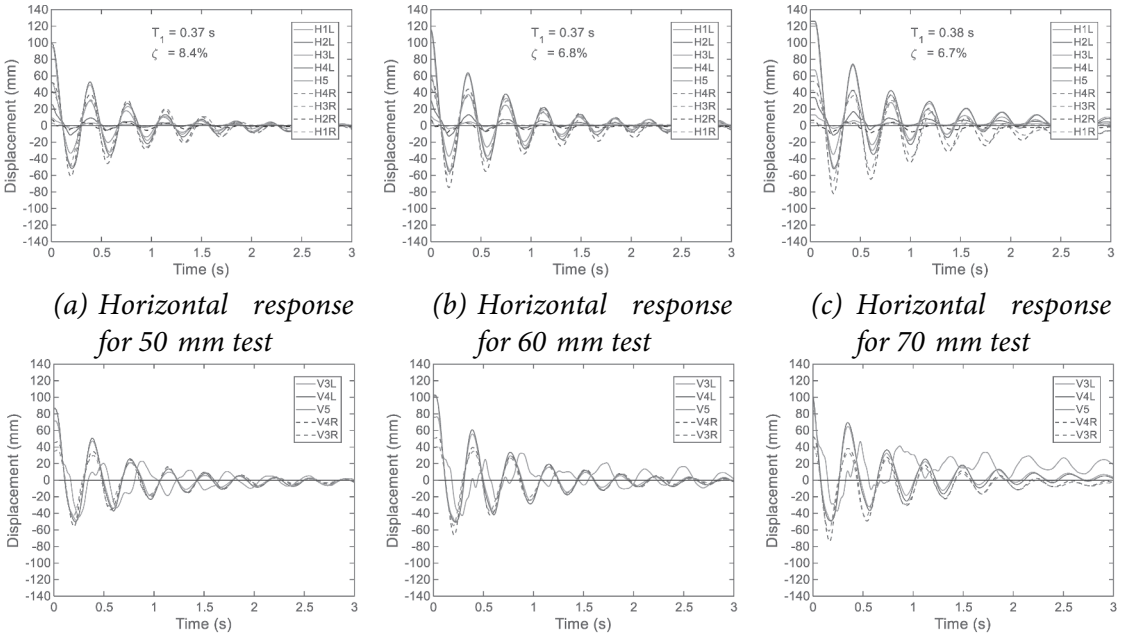

(a) Horizontal response for 50 mm test

(b) Horizontal response for 60 mm test

(c) Horizontal response for 70 mm test

(d) Vertical response for 50 mm test

(e) Vertical response for 60 mm test

(f) Vertical response for 70 mm test

(g) Normalised deformed shape in 50 mm test

(h) Normalised deformed shape in 60 mm test

(i) Normalised deformed shape in 70 mm test

Figure 14. Snap back response (see Figure 8(e) for sensor locations; deformed shapes normalised with respect to sensor H4L).

The natural period T_1 of each snap back test was evaluated as the average increment between the consecutive positive peaks beginning at the second peak Y_2 and ending at the fifth peak Y_5, which resulted in measured first mode periods of $T_1 = 0.37$ s in the 50 mm and 60 mm tests and $T_1 = 0.38$ s in the 70 mm test. The increase in $T_1 = 0.38$ s in the 70 mm test was likely due to the test structure softening from repeated testing. Damping was evaluated via the logarithmic decrement method (Miroslav et al. 2014) also using Y_2 and Y_5, resulting in the logarithmic decrements $\delta_{50} = 1/3 \times \ln(29.8/6.0) = 0.53$ $\delta_{60} = 1/3 \times \ln(37.5/10.4) = 0.43$ and $\delta_{70} = 1/3 \times \ln(42.8/12.1) = 0.42$ and corresponding damping ratios $\zeta_{50} = 0.53 / \sqrt{(4\pi^2 + 0.53^2)} \times 100 = 8.4\%$, $\zeta_{60} = 0.43 / \sqrt{(4\pi^2 + 0.43^2)} \times 100 = 6.8\%$ and $\zeta_{70} = 0.42 / \sqrt{(4\pi^2 + 0.42^2)} \times 100 = 6.7\%$. The damping of the test unit was averaged across the tests and therefore the adopted damping was $\zeta = (8.4 + 6.8 + 6.7)/3 = 7.3\%$. It is noteworthy that damping would be further increased as claddings were added (Devin and Fanning 2019; Ellis and Bougard 2001). Normalised deformed shapes for the first peak Y_1 (corresponding to $T = 0$ s in Figure 14) were established with respect to the largest measured displacement (recorded by sensor H4L) as shown in Figure 14(g-i) and it is evident that the shapes are consistent across all tests.

3.2. Companion numerical models

Two finite element numerical models (FEM) were developed using *SAP2000* (Computers and Structures, Inc 2024), with one model incorporating the full distribution of masses present in the proposed new and resilient meeting house (wharenui) that was used to confirm the first mode period to be used to establish the design earthquake load, and the other model representing a companion numerical model of the test structure that was used to forecast structural response characteristics and internal member actions that were not physically measured during field testing. In both models, the boundary conditions were assumed to be fixed restraints at the base of the columns (poupou), and all member connections are assumed to be pinned. Trials were undertaken to investigate the efficacy of including springs within the numerical models to represent foundation stiffness characteristics and to represent joint rotational characteristics, but it was established that there was no improvement in correlation of modelled versus measured response when compared to the more elegant assumption of a perfectly fixed base condition and pure pinned connections. Member section properties were based on known test unit cross-sectional dimensions, and the material properties for GL8 glulam radiata pine were obtained from NZS 1328.2 (Standards New Zealand 1998), including a density of 550 kg/m^3 and Young's modulus of 8 GPa.

The model used to establish design seismic loading demands incorporated the seismic mass of the absent roof and carvings as shown in Figure 15(a). The proportion of dead and live load concentrated at the ridge beam (tāhuhu) was previously estimated to be G = 14.15 kN and Q = 6.24 kN and therefore the seismic mass applied at the tāhuhu was $G + 0.3Q = 14.15 + 0.3 \times 6.24 = 16$ kN. Similarly, the proportion of dead and live load concentrated at the two semicircular knee joints (ruawhetū) were the loads acting over the remainder of the roof and were previously estimated to be 8.96 kN and 3.96 kN, respectively. The load was shared between the two semicircular knee joints (ruawhetū) and hence the seismic mass applied at each semicircular knee joints (ruawhetū) was $(G + 0.3Q)/2 = (8.96 + 0.3 \times 3.96)/2 = 5$ kN. A modal analysis was undertaken and a fundamental period of $T_1 = 0.37$ s was determined, closely matching the dynamic response measured during in-field testing as reported earlier

The 50 mm snap-back test was simulated using the companion numerical model replicating the as-tested configuration, as shown in Figure 15(b), with the 14.15 kN IBC supplementary vertical load incorporated as a point force acting beneath the centre of the ridge beam (tāhuhu). The post-tensioning was incorporated via a series of thrust forces (P) acting at the semicircular knee joints (ruawhetū), purlins (kaho) and ridge beam (tāhuhu). These thrust forces were evaluated as force resultants using the simplified cosine rule $p = \sqrt{(2F^2(1 - \cos\theta))}$ based on the applied post-tensioning force (F) of 2 kN and the deviation angles (θ) shown in Figure 15(c). At the semicircular knee joints (ruawhetū) $P_R = \sqrt{(2 \times 2^2 \times (1 - \cos 36°))} = 1.24$ kN, at the lower purlins (kaho) $P_3 = \sqrt{(2 \times 2^2 \times (1 - \cos 13°))} = 0.45$ kN, at the upper purlins (kaho) $P_4 = \sqrt{(2 \times 2^2 \times (1 - \cos 16°))} = 0.56$ kN and at the ridge beam (tāhuhu) $P_5 = \sqrt{(2 \times 2^2 \times (1 - \cos 41°))} = 1.4$ kN. In order to generate the 50 mm release horizontal displacement, it was necessary to apply two 16.5° point forces at one-third and two-thirds along the ridge beam (tāhuhu). This combined force was determined to be 89 kN with the vertical and horizontal components being $89 \times \sin 16.5°/2 = 12.5$ kN and $89 \times \cos 16.5°/2 = 42.5$ kN, respectively. Consequently, the base shear force sustained by the test structure in conjunction with the 50 mm snap back test was $42.5 \times 2 = 85.0$ kN, representing 246% of the design-level base shear force demand (V = 34.6 kN). Consequently, it was concluded that the test structure had adequate strength to withstand design earthquake loading.

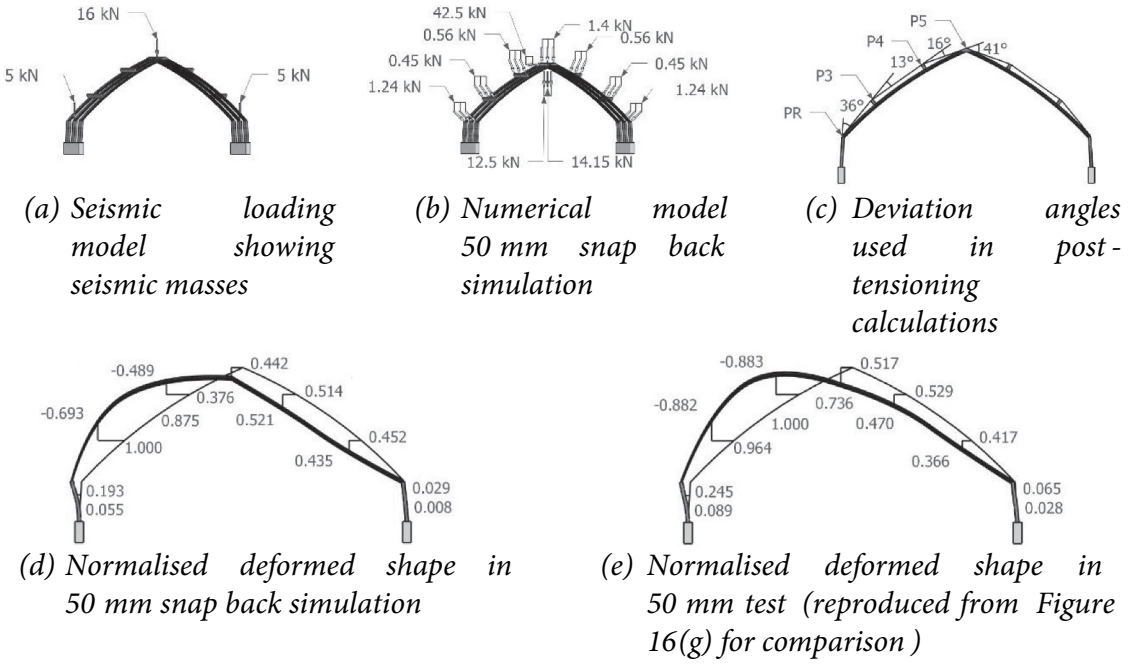

(a) Seismic loading model showing seismic masses

(b) Numerical model 50 mm snap back simulation

(c) Deviation angles used in post-tensioning calculations

(d) Normalised deformed shape in 50 mm snap back simulation

(e) Normalised deformed shape in 50 mm test (reproduced from Figure 16(g) for comparison)

Figure 15. Fem details and response comparison of companion numerical model and test structure response.

The correlation between the simulated and the measured normalised deformed shapes (shown in Figure 15 (d,e) was determined based on the average percentage error (E) across all sensors, where $E = (\Delta_s - \Delta_f)/\Delta_f$, and Δ_s and Δ_f are the simulated and field normalised displacements, respectively. This percentage error was evaluated to be 26% and therefore the correlation was 100–26 = 74%. As previously mentioned, considerable effort was made to align the field and simulated response, and while the match was not exact, the correlation was considered satisfactory to provide indicative values for the internal member actions of the test structure.

The snap back simulation was replicated at the design-level base shear force (V = 34.6 kN) as shown in Figure 16(b), and the resulting axial, shear and bending demands in the columns (poupou) and rafters (heke) were compared to their respective NZS 3603 design member capacities (Standards New Zealand 1993) shown in Figure 16(a). When compared to the demands, it was concluded that the columns (poupou) were loaded to $N_c^*/\varphi N_{nc} = 13.2/1362.9 \times 100 = 1\%$ of their design compression capacity, $V^*/\varphi V_n = 12.2/191.9 \times 100 = 7\%$ of their design shear capacity, and $M^*/\varphi M_n = 20.6/33.3 \times 100 = 62\%$ of their design bending capacity. Similarly, it was concluded that the rafters (heke) were loaded to $N_c^*/\varphi N_{nc} = 23.7/119.6 = 20\%$ of their design compression capacity, $V^*/\varphi V_n = 2.3/109.2 \times 100 = 3\%$ of their design shear capacity, and $M^*/\varphi M_n = 4.6/20.3 \times 100 =$ 23% of their design bending capacity. These results confirmed that the members had considerable strength reserves when subjected to design earthquake loading. A subsequent analysis was undertaken using the 2500-year maximum credible earthquake (MCE) scenario (King and Jury 2001) where the return period factor becomes 1.8 and the corresponding elevated base shear force $V = (1.8/1.3) \times 34.6$ kN = 47.8 kN as shown in Figure 16(c). Because the 50 mm snap back test corresponded with a base shear force of 85.0 kN, it was concluded that the test structure had been subjected to loading well in excess of the MCE scenario.

The code-defined vertical and horizontal displacement limits were previously reported to be 44 mm and 162 mm, respectively. When subject to the design earthquake load the vertical displacement was V5 = 24.7 mm and the horizontal displacement was H5 = 20.3 mm as shown in Figure 17. These displacements represented 24.7/44 = 57% of the vertical limit and 20.3/162 = 13% of the horizontal limit, and it was concluded that the structure had adequate displacement capacity at the design earthquake load.

In order to further investigate member performance, the 70 mm snap back test was subsequently simulated. This simulation resulted in a base shear force V = 119.5 kN which was significantly larger than the MCE scenario. Comparing the resulting demands shown in Figure 18(a) to their respective NZS 3603 design member capacities shown in Figure 16(a) indicated that the columns (poupou) and rafters (heke) did not reach

	Column (Poupou)	Rafter (Heke)
Demands		
N_c^* (kN)	13.2	23.7
V^* (kN)	12.2	2.3
M^* (kNm)	20.6	4.6
$N_{c,MCE}$ (kN)	15.6	28.8
V_{MCE} (kN)	15.3	3.0
M_{MCE} (kNm)	25.7	6.2
Capacities		
ϕN_{nc} (kN)	1362.9	119.6
ϕV_n (kN)	191.9	109.2
ϕM_n (kNm)	33.3	20.3

(a) Design and MCE scenario demands and NZS 3603 design member capacities

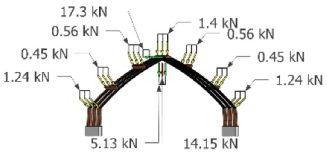

(b) Design earthquake simulation

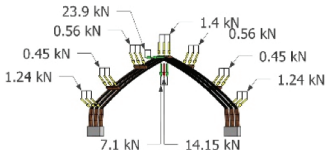

(c) MCE scenario simulation

Figure 16. Design earthquake and MCE scenario simulation demands and NZS 3603 design member capacities.

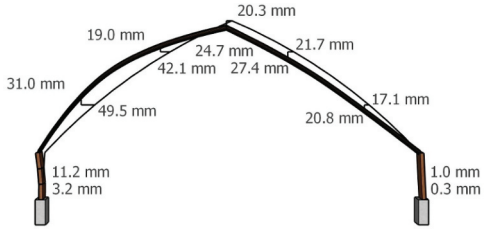

Figure 17. Deformed shape in design earthquake simulation.

failure except for bending in the columns (poupou) where $M_{70}/\varphi M_n = 53.3/33.3 \times 100 = 160\%$. Because no damage was made to the test structure during the 70 mm snap back test, the columns (poupou) being loaded to 160% of their design bending capacity prompted consideration of a strength reserve likely attributable to their overstrength bending capacity M_O. When compared to the design bending capacity φM_n that incorporates the strength reduction factor $\varphi = 0.8$ and characteristic bending stress $f_b = 19$ MPa, M_O omits the strength reduction factor (hence $\varphi = 1$) and uses the mean bending stress $f_{b,mean}$. The study by Milner (2004) contains values for GL13 softwood glulam bending stress supplied across six manufacturers and the average characteristic-to-mean improvement was estimated to be 1.32. For the purposes of this study, this value was assumed to be applicable to GL8 glulam, resulting in $f_{b,mean} = 1.32 \times 19 = 25.1$ MPa and hence $M_O = k_1 k_4 k_{8(b)} f_{b,mean} Z = 1 \times 1.31 \times 1 \times 25.1 \times 0.0017 \times 1000 = 55.0$ kNm. When compared to the bending demand, it was concluded that in reality the columns (poupou) were likely loaded to $M_{70}/M_O = 53.3/55.0 = 97\%$ of their overstrength bending capacity. Therefore, although no damage was made to the test structure during the 70 mm snap back test, bending failure of the column (poupou) was likely imminent with any further displacement.

3.3. Parametric analysis using the companion numerical model

Post-tensioning (mīmiro) was incorporated into the test structure in recognition of its discovery within the archaeological findings at Te Kōhika (the Māori village located near Whakatāne). As a post-tensioning technique associated with canoe (waka) construction, its seafaring origin was also recognised by intentionally sourcing all post-tensioning hardware from the maritime sailing industry. When compared to studies involving more conventional post-tensioning systems that employ higher-capacity steel cables and anchorage hardware and apply post-tensioning forces ranging

	Column (Poupou)	Rafter (Heke)
Demands		
$N_{c,70}$ (kN)	28.7	56.9
V_{70} (kN)	31.7	7.0
M_{70} (kNm)	53.3	15.1
Capacities		
M_O (kNm)	55.0	33.6

(a) 70 mm snap back demands and overstrength bending capacity

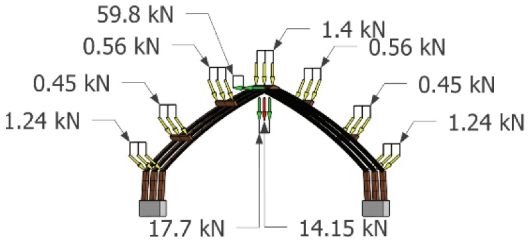

(b) 70 mm snap back simulation

Figure 18. 70 mm snap back simulation demands with overstrength bending capacity.

between 100 kN and 1000 kN (Iqbal, Pampanin, and Buchanan 2015; Ponzo et al. 2019; Wanninger and Frangi 2016), it is plausible that a conventional approach would have resulted in a post-tensioning force significantly larger than F = 2 kN being applied. Therefore, it was of interest to use the companion numerical model to explore the effect of increasing the post-tensioning force.

In the previously mentioned studies, the post-tensioning axial compressive stress was on average equivalent to approximately 7% of the characteristic compressive strength f_c. Based on $f_c = 24$ MPa for GL8 as obtained from Techlam (2021) and the rafter (heke) cross-sectional area $(\pi \times 165^2)/(2 \times 1000^2) = 0.043\ m^2$ (dimensions shown in Figure 3(d)) the equivalent post-tensioning cable force for the test structure would be $F = 0.07 \times 24 \times 0.043 \times 1000 = 72$ kN. Consequently, the design-level base shear demand (V = 34.6 kN) was first applied to a model that incorporated a post-tensioning force of F = 70 kN (referred to hereafter as the 35F simulation as shown in Figure 19(b) and the resulting member actions shown in Figure 19(a) were compared to those of the as-tested numerical model (hereafter referred to as F simulation) also previously reported in Figure 16(a). When subject to 35 F, it was concluded that the columns (poupou) demands increased by $(N_{c,35F}^*\text{-}N_c^*)/N_c^* = (53.4 - 13.2)/13.2 = 305\%$ for axial compression, $(V_{35F}^*\text{-}V^*)/V^* = (16.6 - 12.2)/12.2 = 37\%$ for shear and $(M_{35F}^*\text{-}M^*)/M^* = (27.9 - 20.6)/20.6 = 36\%$ for bending. Similarly, it was concluded that the rafter (heke) demands increased by $(N_{c,35F}^*\text{-}N_c^*)/N_c^* = (86.7 - 23.7)/23.7 = 266\%$ for axial compression, $(V_{35F}^*\text{-}V^*)/V^* = (8.7 - 2.3)/2.3 = 279\%$ for shear and $(M_{35F}^*\text{-}M^*)/M^* = (16.3 - 4.6)/4.6 = 255\%$ for bending. Despite these elevated demands, the design member capacities of the columns (poupou) and rafters (heke) were not exceeded and hence it was concluded that the test structure had adequate strength to withstand design earthquake loading in conjunction with more conventional levels of post-tensioning. As shown in Figure 19 the apex horizontal displacement in all simulations remained 20.3 mm and therefore it was concluded that F had no significant influence on horizontal stiffness at the apex. The comparison between the F and 35 F deformed shapes shown in Figure 19(c) and (d) illustrated that increasing F caused progressive sag in the rafters (heke), occurring asymmetrically and disproportionately affecting the right rafters (heke) due to the design-level base shear force. When considering the centre of the rafters (heke) the resultant displacements in the F simulation were a $\sqrt{(31.1^2 + 49.7^2)} = 58.6$ mm hog at the left rafters (heke) and a $\sqrt{(24.2^2 + 19.6^2)} = 31.2$ mm sag at the right rafters (heke), corresponding to a total imbalance of 58.6 + 31.2 = 89.8 mm. Similarly, in the 35 F simulation, these displacements were a $\sqrt{(39.9^2 + 45.1^2)} = 60.2$ mm sag at the left rafters (heke) and a $\sqrt{(95.2^2 + 114.4^2)} = 148.8$ mm sag at right rafters (heke), corresponding to a total imbalance of 148.8 - 60.2 = 88.6 mm. The optimal post-tensioning force was determined to be the value that balanced these rafter (heke) midspan displacements. Consequently, parametric analysis was undertaken, and this value was determined to be 5 F (or alternatively 10 kN) where the resultant displacements were a $\sqrt{(22.7^2 + 38.5^2)} = 44.7$ mm hog at the right rafters (heke) and a $\sqrt{(32.6^2 + 30.7^2)} = 44.8$ mm sag at the right heke as shown in Figure 19(e).

	Column (Poupou)	Rafter (Heke)
Peak member actions		
$N_{c,35F}^*$ (kN)	53.4	86.7
V_{35F}^* (kN)	16.6	8.7
M_{35F}^* (kNm)	27.9	16.3

(a) 35F simulation demands

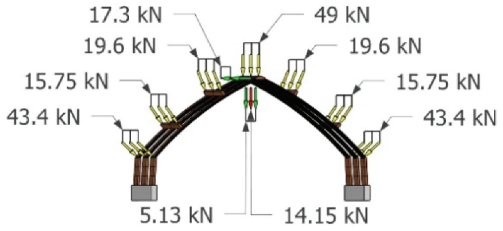

(b) 35F simulation

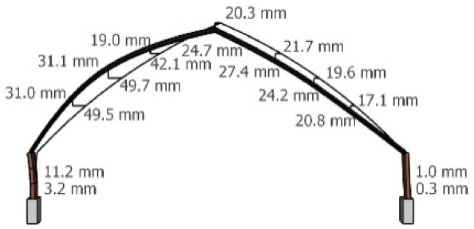

(c) Deformed shape in F simulation

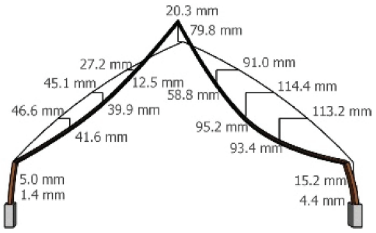

(d) Deformed shape in 35F simulation

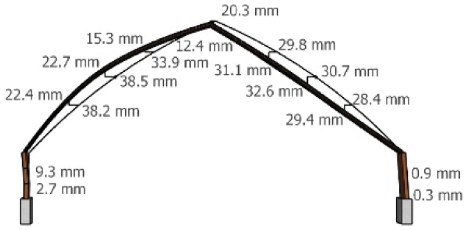

(e) Deformed shape in 5F simulation

Figure 19. 50 mm snap back test and 35F simulation demands and comparison of deformed shapes.

4. Conclusions

Field testing of a full-scale post-tensioned glue laminated timber portal frame structure was undertaken at a test site located near Ōpōtiki in the eastern Bay of Plenty region of New Zealand. The following conclusions were made in relation to the reported research:

(1) The vertical and horizontal loading systems were trialled in the laboratory and at a nearby off-site location before being applied in the field located approximately 350 km away from home base. This exercise significantly improved preparation and is recommended for projects with similar conditions.
(2) The simulated seismic response was consistent across all tests except for measurements recorded at sensor V5, which was likely disrupted by vertical bouncing motion of the IBCs as a result of the non-horizontal orientation of the loading system.
(3) From snap back testing, the first mode period was $T_1 = 0.37$ s with 7.3% damping and consistent normalised deformed shapes, noting that damping would be further increased as claddings were added.
(4) The design-level base shear demand was V = 34.6 kN and the MCE demand were 47.8 kN. The maximum base shear force sustained during testing was V = 85.0 kN, demonstrating that the test structure withstood design and MCE earthquake loading.
(5) Satisfactory correlation (74%) was achieved between the test structure and the companion numerical model.
(6) For the design-level base shear force V = 34.6 kN simulation: the columns (poupou) were loaded to 1% in compression ($\varphi N_{nc} = 1362.9$ kN), 7% in shear ($\varphi V_n = 191.9$ kN) and 62% in bending ($\varphi M_n = 33.3$ kNm); the rafters (heke) were loaded to 20% in compression ($\varphi N_{nc} = 119.6$ kN), 3% in shear ($\varphi Vn = 109.2$ kN) and 23% in bending ($\varphi Mn = 20.3$ kNm); and displacements reached 57% and 13% of the vertical and horizontal limits, respectively.
(7) For the 70 mm snap back test simulation: the columns (poupou) were loaded to 160% of the design-level bending capacity and 97% of their overstrength bending capacity. It was concluded that the columns (poupou) members were tested to their full limit without failure.

(8) The applied post-tension force (F) of 2 kN was dictated by the low-technology procedures intentionally adopted. Using parametric analysis, it was determined from the companion numerical model that a post-tension force of 10 kN would have resulted in optimally reduced peak deformations for the rafters (heke).

Acknowledgement

Community: Ngāti Ira o Waioweka is thanked for their trust in allowing the research team to be the conveyors of this research about their ancestral house (tīpuna) and allowing structural testing to occur on their marae. Mangai (spokesperson) Roger Riki and researcher Anna Marei-Kurei. Riki and Cheryl Kurei from Kurei Mahi Partners. The passing of their son Wiremu Kurei who participated in the research is acknowledged and much love (aroha nui) is extended to the bereaved family (whānau pani). From Hoete's iwi, Ngāti Awa, Reuban Araroa (CEO), Romana Graham (GM People & Capability) and Mike Panapa (Cultural Advisor), and kaumātua (elder) Aubrey Hōete.

Industry: Alistair Cattanach (Dunning Thornton) for timber engineering design and specification, John & Clark Hunia (Rāwhiti East Coast Scaffolding Ltd.) for installation of the structure, Andrew Hewitt (RedStag TimberLab) for the supply of the engineered timber elements, Peter Vitali (Fosters Chandlery Harken NZ) for sailing equipment specification, and Ngārchitecture Ltd (new Māori architecture).

University of Auckland: Dr Jeremy Treadwell for his pioneering thesis Tuia Te Whare: The Culture of Māori Architectural Technology, Dr Mike Austin for expertise on Polynesian ocean voyaging vessels, Zane Egginton (digital research technologies), Denice Belsten and Melanie Milicich (research management), James Corles, Oscar Botha, Kimberley Fernandes, Naomi Felicia, and Sam Julian. At the UoA Structures Testing Laboratory, Geoff Kirby (Senior Technician) and Mark Byrami (Technician) for the field-testing trailer. Josh Kirby for site set-out assistance. Professor Liam Wotherspoon is thanked for providing the equipment used in hand shear vane testing.

Disclosure statement

In accordance with Taylor & Francis policy and standard ethical guidelines for research transparency, the authors confirm that they have no relevant financial or non-financial competing interests to declare. The authors have no affiliations, funding relationships, personal fees, professional roles, access arrangements, or other associations that could be perceived as influencing the work reported herein.

Funding

New Zealand's Natural Hazards Commission Toka Tu Ake Biennial Grants Programme funded Mīmirū: The application of an endangered indigenous construction practice onto prototype timber portals to assess seismic resilience with Professor Anthony Hōete as Principal Investigator (Natalie Balfour, Hema Wihongi and Coen Lammers). QuakeCoRE is New Zealand's Centre for Research Excellence in Seismic Resilience and funded Disciplinary Theme 5 which undertook community-oriented and co-designed research with the aim to innovate mātauranga Māori (Māori knowledge) that supports the earthquake resilience aspirations of tangata whenua. Hōete's Research Development Account at the University of Auckland.

ORCID

Sonny Vercoe http://orcid.org/0009-0008-4740-165X
Anthony Hōete http://orcid.org/0000-0003-0103-9831
Jason Ingham http://orcid.org/0000-0002-0989-9097
Sherif Beskhyroun http://orcid.org/0000-0003-1799-1018

References

Auckland Off Road Adventure. 2024. *Auckland Off Road Adventure*. Auckland Off Road Adventure. https://aucklandoffroadadventure.com/.

Buchanan, A., S. Pampanin, M. Newcombe, and A. Palermo. 2009. "Non-Conventional Multi-Storey Timber Buildings Using Post-Tensioning." In *Proceedings of the 11th International Conference on Non-Conventional Materials and Technologies*, 30. University of Bath, Bath, UK.

Chang, W.-S., and M.-F. Hsu. 2010. "Full-Scale Experiment on Reinforced Taiwanese Traditional Timber Frames." In *11th World Conference on Timber Engineering 2010, WCTE 2010, 4*, Riva del Garda, Trentino, Italy, 20–24 June 2010. Finnish Association of Civil Engineers.

Computers and Structures, Inc. 2024. *SAP2000 Structural Analysis and Design*. CSI America. https://www.csiamerica.com/products/sap2000.

Devin, J., and P. Fanning. 2019. "Experimental Investigation of the Contribution of Cladding Panels to the Seismic Response of Reinforced Concrete Buildings." *Engineering Structures* 197: 109420.

Ellis, B. R., and A. Bougard. 2001. "Dynamic Testing and Stiffness Evaluation of a Six-Storey Timber-Framed Building." *Engineering Structures* 23 (7): 790–801.

Engineering Design Consultants Limited. 2023. *Ground Bearing Assessment 21 Waioeka Pā Road Ōpōtiki*.

Fosters Chandlery. 2024a. *Fineline Classic Double Braid*. Fosters Chandlery. https://fostersshipchandlery.co.nz/products/fineline-classic-double-braid.

Fosters Chandlery. 2024b. *Nylon Horn Cleat*. Fosters Chandlery. https://fostersshipchandlery.co.nz/products/cleat-horn-nylon-black-115mm.

GNS Science. 2024. *Geological Map of New Zealand*. GNS Science Te Pū Ao. https://www.gns.cri.nz/data-and-resources/geological-map-of-new-zealand/.

Harken New Zealand, Limited. 2024a. *8 Plain-Top Classic Winch—Aluminum*. Harken. http://www.harken.co.nz/en/shop/classic/8-plain-top-classic-winch-aluminum/.

Harken New Zealand, Limited. 2024b. *45mm Aluminum Element Block—Swivel*. Harken Marine. http://www.harken.co.nz/en/shop/element-blocks/45-mm-aluminum-element-block-swivel/ .

Harken New Zealand, Limited. 2024c. *98mm Diamond Padeye*. Harken. http://www.harken.co.nz/en/shop/fixed-padeyes/98-mm-diamond-padeye/.

Harken New Zealand, Limited. 2024d. *Aluminum Lock-In Winch Handle—254mm*. Harken. http://www.harken.co.nz/en/shop/aluminum-chrome-bronze-winch-handles/aluminum-lock-in-winch-handle-254-mm/ .

Hoete, A. 2020. "The House as Ancestor: A Tale of Māori Social Value." *Archit. Design* 90: 112–119. https://doi.org/10.1002/ad.2598.

Hoete, A. 2025. MIMIRU: The Application of an Endangered Indigenous Construction Practice Onto Prototype Timber Portals to Assess Seismic Resilience. Natural Hazards Commission Toka Tū Ake. https://www.naturalhazards.govt.nz/assets/Publications-Resources/241202_Hoete_Mimiru_Report-Natural-Hazards-Toka-Tu-Ake.pdf.

Iqbal, A., S. Pampanin, and A. Buchanan. 2021. "A General Design Approach for Post-Tensioned Timber Subassemblies." *Journal of Earthquake Engineering* 25 (14): Article 14. https://doi.org/10.1080/13632469.2019.1659880

Iqbal, A., S. Pampanin, and A. H. Buchanan. 2015. "Seismic Performance of Full-Scale Post-Tensioned Timber Beam-Column Connections." *Journal of Earthquake Engineering* 20 (3): 383–405. https://doi.org/10.1080/13632469.2015.1070386

Kasal, B., S. Pospisil, I. Jirovsky, A. Heiduschke, M. Drdacky, and P. Haller. 2004. "Seismic Performance of Laminated Timber Frames with Fiber-Reinforced Joints." *Earthquake Engineering & Structural Dynamics* 33 (5): 633–646. https://doi.org/10.1002/eqe.368

King, A. B., and R. D. Jury. 2001. "Future Earthquake Loadings Standards." Paper presented at the NZSEE 2001 Conference, Wairakei Resort, Taupō, New Zealand. https://www.nzsee.org.nz/db/2001/papers/60101paper.pdf .

Komatsu, K. 1993. "Mechanical Timber Joints and Their Application to Glulam Portal Frames." *Recent Research on Wood and Wood-Based Materials*: 109–118. https://doi.org/10.1016/B978-1-4831-7821-9.50017-4

Komatsu, K. 2017. "Development of Stiffer and Ductile Glulam Portal Frame." *AIP Conference Proceedings* 1903 (1): 020026. https://doi.org/10.1063/1.5011506

Komatsu, K., and T. Mori. 2006. "Development of Ductile and High-Strength Semi-Rigid Portal Frame Composed of Mixed-Species Glulams and H-Shaped Steel Gusset Joints." *Sustainable Humanosphere: Bulletin of Research Institute for Sustainable Humanosphere Kyoto University* (2):10.

Liu, Y., and H. Xiong. 2018. "Lateral Performance of a Semi-Rigid Timber Frame Structure: Theoretical Analysis and Experimental Study." *Journal of Wood Science* 64 (5): 591–600. https://doi.org/10.1007/s10086-018-1727-7

Milner, H. R. 2004. *Design Values for Australian Glulam*. Forest Wood Products Research and Development Corporation. https://fwpa.com.au/wp-content/uploads/2004/04/PN01.3700.pdf#:~:text=Mean%2038,Normalized%20characteristic%20bending%20strength%20Rk%2Cnorm.

Ministry of Business, Innovation & Employment. 2023. *Verification Method B1/VM4: Foundations*. November 2. https://www.building.govt.nz/assets/Uploads/building-code-compliance/b-stability/b1-structure/asvm/b1-structure-1st-edition-amendment-21.pdf.

Miroslav, J., A. Simonovic, N. Zorić, and N. Lukić. 2014. "Experimental Determination of Active Structure Damping Ratio Using Different Control Strategies in System of Active Vibration Control." ResearchGate. 6th International Scientific Conference on Defensive Technologies, OTEH, Belgrade, Serbia. October. https://www.researchgate.net/publication/266673188_EXPERIMENTAL_DETERMINATION_OF_ACTIVE_STRUCTURE_DAMPING_RATIO_USING_DIFFERENT_CONTROL_STRATEGIES_IN_SYSTEM_OF_ACTIVE_VIBRATION_CONTROL.

Moroder, D., A. H. Buchanan, and S. Pampanin. 2013. "Preventing Seismic Damage to Floors in Post-Tensioned Timber Frame Buildings." Preventing Seismic Damage to Floors in Post-Tensioned Timber Frame Buildings. New Zealand Society of Earthquake Engineering Conference, Wellington. https://www.nzsee.org.nz/db/2013/Paper_57.pdf.

Ngāti Ira, 2022. "Tanewhinaki. Booklet distributed at Te Wānanga Hapū o Ngāti Ira ki Ōpeke Marae."

Ni, C., M. Mohammad, A. Al Mamun, and G. Doudak. 2014. "Performance Evaluation of Portal Frame System in Low-Rise Light-Frame Wood Structures." *Journal of Structural Engineering* 140 (3): Article 3. https://doi.org/10.1061/(ASCE)ST.1943-541X.0000878

Noguchi, M., S. Takino, and K. Komatsu. 2006. "Development of Wooden Portal Frame Structures with Improved Columns." *Journal of Wood Science* 52 (1): 51–57. https://doi.org/10.1007/s10086-005-0714-y

Palermo, A., S. Giorgini, P. Stefano, and A. H. Buchanan. 2011. "Potential of Longitudinal Post-Tensioning for Short-to-Medium Span Timber Bridges." *Structural Engineering International* 21 (3): 349–355. https://doi.org/10.2749/101686611X13049248220320

Palermo, A., S. Pampanin, A. Buchanan, and M. Newcombe. 2005. "Seismic Design of Multi-Storey Buildings Using Laminated Veneer Lumber (LVL)." Paper presented at the NZSEE 2005 Annual Conference, Wairakei Resort, Taupō, New Zealand, 11–13. March. https://ir.canterbury.ac.nz/server/api/core/bitstreams/59d4d7a0-f6aa-4ca1-af3a-181ecd59d74b/content.

Ponzo, F. C., A. Di Cesare, N. Lamarucciola, and D. Nigro. 2019. "Seismic Design and Testing of Post-Tensioned Timber Buildings with Dissipative Bracing Systems." *Frontiers in Built Environment* 5:5. https://doi.org/10.3389/fbuil.2019.00104

Ronstan International Pty Ltd. 2024. *Series 50 High Load Exit Box*. Ronstan. https://www.ronstan.com/s50-hl-exit-boxsinglesuits-rope-wire.html.

Shahmohammadi, A., J. B. P. Lim, C. Clifton, and M. Hajsadeghi. 2022. "Full-Scale Experimental Tests on Portal Frames Comprising Novel Cold-Formed Tapered Box Sections." *Journal of Structural Engineering* 148 (9): 04022133. https://doi.org/10.1061/(ASCE)ST.1943-541X.0003379

Smith, T., D. Carradine, A. Di Cesare, F. Ponzo, S. Pampanin, A. Buchanan, and D. Nigro. 2012. "Experimental Investigations of Post-Tensioned Timber Frames with Advanced Seismic Damping Systems." *Experimental Investigations of Post-Tensioned Timber Frames with Advanced Seismic Damping Systems*: 1745–1754. https://doi.org/10.1061/9780784412367.154

Smith, T., F. C. Ponzo, A. Di Cesare, S. Pampanin, D. Carradine, A. H. Buchanan, and D. Nigro. 2014. "Post-Tensioned Glulam Beam-Column Joints With Advanced Damping Systems: Testing and Numerical Analysis." *Journal of Earthquake Engineering* 18 (1): 147–167. https://doi.org/10.1080/13632469.2013.835291

Spellman, P. M., A. K. Abu, D. M. Carradine, P. J. Moss, and A. H. Buchanan. 2012. "Design of Post-Tensioned Timber Beams for Fire Resistance." Proceedings of the 7th International Conference on Structures in Fire. International Conference on Structures in Fire, Zürich. http://hdl.handle.net/10092/7384 .

Spinlock Limited. 2024. *XAS Effortless Multi-Role Clutch*. Spinlock. https://www.spinlock.co.uk/en-GB/uk/products/xas .

Standards New Zealand. 1993. *NZS 3603:1993*. September 21. https://www.standards.govt.nz/shop/NZS-36031993 .

Standards New Zealand. 1998. *AS/NZS 1328: 1998*. https://www.standards.govt.nz/shop/asnzs-1328-21998/ .

Standards New Zealand. 2002a. *AS/NZS 1170.0: 2002*. June 3. https://www.standards.govt.nz/shop/asnzs-1170-02002.

Standards New Zealand. 2002b. *AS/NZS 1170.1: 2002*. June 3. https://www.standards.govt.nz/shop/asnzs-1170-12002.

Standards New Zealand. 2004. *NZS 1170.5: 2004: Standards New Zealand*. https://www.standards.govt.nz/shop/nzs-1170-52004/ .

Standards New Zealand. 2011. August 1). *NZS 3604:2011*. https://www.standards.govt.nz/shop/nzs-36042011/ .

Techlam. 2021. *Techlam Glulam Specifications & Characteristics*. February. https://techlam.nz/wp-content/uploads/2018/04/17739_GlulamSpecsandCharacteritics-February-2021.pdf.

VPG Force Sensors. 2024. *Universal Load Cell Model 9363*. https://docs.vpgforcesensors.com/?id=2770&_gl=1*1u677k3*_ga*MTU3NTI5ODUyMC4xNjk4MjAxNTI2*_ga_JVJNRP2P4F*MTY5ODIwMjI5My43LjAuMA.

Wanninger, F., and A. Frangi. 2016. "Experimental and Analytical Analysis of a Post-Tensioned Timber Frame Under Horizontal Loads." *Engineering Structures* 113:16–25. https://doi.org/10.1016/j.engstruct.2016.01.029

Wikipedia. 2024a. "1886 Eruption of Mount Tarawera." https://en.wikipedia.org/w/index.php?title=1886_eruption_of_Mount_Tarawera&oldid=1253275619.

Wikipedia. 2024b. "1931 Hawke's Bay Earthquake." https://en.wikipedia.org/w/index.php?title=1931_Hawke%27s_Bay_earthquake&oldid=1253672175.

Xiong, H., and Y. Liu. 2016. "Experimental Study of the Lateral Resistance of Bolted Glulam Timber Post and Beam Structural Systems." *Journal of Structural Engineering* 142 (4): E4014002. https://doi.org/10.1061/(ASCE)ST.1943-541X.0001205

Yeap, K. S., and D. E. C. Yeoh. 2022. "A Comprehensive Research Review on Timber Post-Tensioning Technology." *Recent Trends in Civil Engineering and Built Environment* 3 (1): Article 1.

Zhang, C., H. Guo, K. Jung, R. Harris, and W.-S. Chang. 2019. "Using Self-Tapping Screw to Reinforce Dowel-Type Connection in a Timber Portal Frame." *Engineering Structures* 178:656–664. https://doi.org/10.1016/j.engstruct.2018.10.066